Edaravone leads to proteome changes indicative of neuronal cell protection in response to oxidative stress

Mohammad-Saeid Jami [a, d], Zahra Salehi-Najafabadi [a], Fereshteh Ahmadinejad [d], Esthelle Hoedt [b], Morteza Hashemzadeh Chaleshtori [d], Mahdi Ghatrehsamani [d], Thomas A. Neubert [b], Jan Petter Larsen [c], Simon Geir Møller [a, c, *]

[a] Department of Biological Sciences, St John's University, New York, NY, USA
[b] Kimmel Center for Biology and Medicine at the Skirball Institute and Department of Biochemistry and Molecular Pharmacology, New York University School of Medicine, New York, NY, USA
[c] The Norwegian Centre for Movement Disorders, Stavanger University Hospital, Norway
[d] Cellular and Molecular Research Center, Shahrekord University of Medical Sciences, Shahrekord, Iran

ARTICLE INFO

ABSTRACT

Neuronal cell death, in neurodegenerative disorders, is mediated through a spectrum of biological processes. Excessive amounts of free radicals, such as reactive oxygen species (ROS), has detrimental effects on neurons leading to cell damage via peroxidation of unsaturated fatty acids in the cell membrane. Edaravone (3-methyl-1-phenyl-2-pyrazolin-5-one) has been used for neurological recovery in several countries, including Japan and China, and it has been suggested that Edaravone may have cytoprotective effects in neurodegeneration. Edaravone protects nerve cells in the brain by reducing ROS and inhibiting apoptosis. To gain further insight into the cytoprotective effects of Edaravone against oxidative stress condition we have performed comparative two-dimensional gel electrophoresis (2DE)-based proteomic analyses on SH-SY5Y neuroblastoma cells exposed to oxidative stress and in combination with Edaravone. We showed that Edaravone can reverse the cytotoxic effects of H_2O_2 through its specific mechanism. We observed that oxidative stress changes metabolic pathways and cytoskeletal integrity. Edaravone seems to reverse the H_2O_2-mediated effects at both the cellular and protein level via induction of Peroxiredoxin-2.

© 2015 Elsevier Ltd. All rights reserved.

1. Introduction

Neurodegeneration is characterized by the progressive death of neurons. Neurodegenerative processes cause many neurodegenerative disorders including Parkinson's disease (PD), Amyotrophic lateral sclerosis (ALS), Huntington's disease (HD), and Alzheimer's diseases (AD). For instance, PD is the most common neurodegenerative movement disorder, which affects approximately 1% of individuals above 60 years of age, and is characterized by cumulative neuronal loss (De Lau and Breteler, 2006). Due to the increase in the aging population the prevalence of PD is very likely to double within the next two decades (Dorsey et al., 2007). The preferential dopaminergic neuronal cell death in the substantia nigra results in reduced dopamine levels in the striatum, which causes the motor symptoms associated with PD. At clinical diagnosis this region of the brain has irreversibly lost 50–70% of its neurons compared to unaffected individuals (Davie, 2008).

Free radicals, like reactive oxygen species (ROS), play a crucial role in neurodegeneration and brain injury by exacerbating neuronal cell membrane damage via peroxidation of unsaturated fatty acids. Since the substantia nigra of PD patients exhibit higher levels of oxidized lipids (Bosco et al., 2006), proteins and DNA (Nakabeppu et al., 2007), and lower levels of reduced glutathione (GSH) (Zeevalk et al., n.d.), oxidative stress and mitochondrial dysfunction are known to be potential integrated causes of neurodegeneration in PD (Dawson et al., 2010).

* Corresponding author. Department of Biological Sciences, St John's University, New York, NY, USA. Tel: +1 718 990 3917; fax: +1 718 990 1894.
E-mail addresses: sjamif@gmail.com (M.-S. Jami), Zahra.salehi@live.com (Z. Salehi-Najafabadi), Fereshte.ahmadi86@ymail.com (F. Ahmadinejad), Esthelle.Hoedt@med.nyu.edu, esthellehoedt@gmail.com (E. Hoedt), mchalesh@yahoo.com (M.H. Chaleshtori), Thomas.Neubert@med.nyu.edu (T.A. Neubert), jpl@sus.no (J.P. Larsen), mollers@stjohns.edu (S.G. Møller).

Although neuroprotection and recanalization are main neurodegenerative disease treatment targets, the only current symptomatic approach for treating PD is based on a dopamine replacement strategy, using the dopamine precursor L-3,4-dihydroxyphenylalanine (L-Dopa), which at best only alleviates the motor symptoms. It is known that L-Dopa can also damage dopaminergic (DA) neurons (Blessing et al., 2003; Mena et al., 2009) as chronic treatment is associated with the development of complications such as dyskinesia, motor fluctuation, and dementia (Liu et al., 2014).

Recently a number of studies have focused on developing alternative neuroprotective therapeutic approaches with the ultimate aim of potentially slowing down neurodegeneration. In several countries, including Japan and China, Edaravone (3-methyl-1-phenyl-2-pyrazolin-5-one) has been widely used during the last decade for neurological recovery following acute brain ischemia and subsequent cerebral infarction (Lapchak, 2010). This neuroprotective drug acts as a potent antioxidant protecting against oxidative stress and neuronal apoptosis (Kikuchi et al., 2011; Yoshida et al., 2006) and its beneficial effects has been studied in several clinical trials (Kikuchi et al., 2014). Indeed it has been shown that oxidative cell damage in rat brain is reduced by repeated Edaravone treatment (Yamamoto et al., 2009). Moreover, other studies on HT22 cells demonstrated that Edaravone protects against H_2O_2-induced injury by inhibiting the production of ROS and activating the MAPK signaling pathway (Zhao et al., 2013). Edaravone has lipophilic groups, exhibiting good cell membrane permeability and the ability to cross the blood–brain barrier. Recent studies show that Edaravone protects brain nerve cells by reducing ROS, inhibiting apoptosis, blocking non-enzymatic peroxidation and lipoxygenase activity, and preventing vascular endothelial cell injury (Shinohara and Inoue, 2013). These findings suggest that Edaravone may have value in the treatment of neurodegenerative disorders such as PD.

In our previous study we performed a comparative two-dimensional gel electrophoresis (2DE)-based proteomic analysis to gain further insight into the effects of L-DOPA in response to H_2O_2-mediated oxidative stress in SH-SY5Y neuronal cells. We showed that exposure to L-DOPA may aid hypoxia condition in cells and therefore induction of ORP150 (hypoxia up-regulated protein 1) with its concomitant cytoprotective effects (Jami et al., 2014b). Here we have performed a similar study to analyze the cytoprotective effects of Edaravone. We have shown that similar to L-DOPA, Edaravone can reverse the cytotoxic effects of H_2O_2 but through a different mechanism.

2. Material and methods

2.1. Reagents and cell culture

Fetal bovine serum (FBS), phosphate buffered saline (PBS), Dulbecco's minimum essential medium plus F12 (DMEM/F12), penicillin and streptomycin were purchased from Invitrogen (Gaithersburg, MD). Acrylamide/bis-acrylamide, tris base, glycine, ammonium persulfate, PVDF membrane, TEMED, DTT, SDS, urea, thiourea, glycerol, ammonium bicarbonate, DMSO, ECL reagent, bromoplenol blue were purchased from Fisher Scientific (Pittsburgh, PA). Trypsin and trypan blue were obtained from Sigma–Aldrich (St. Louis, MO).

SH-SY5Y cells were cultured in DMEM/F12 containing 10% FBS, 100 U/ml penicillin and 100 mg/ml streptomycin at 37 °C in an atmosphere containing 5% CO_2. In order to perform treatments the media were supplemented with 2 mM H_2O_2 (Sigma–Aldrich, MO), 25 μM Edaravone (Abcam, MA) or a combination of H_2O_2/Edaravone for 8 h (Kaste et al., 2013).

2.2. Lactate dehydrogenase (LDH) cytotoxicity assay

Cellular damage following each treatment condition was assessed by measurement of LDH released into the medium. At the end (8 h) of each treatment, 50 μl of medium was collected and transferred to a 96-well plate. The measurement of LDH reaction level was performed using the Pierce LDH Cytotoxicity Assay Kit (Thermo Scientific, USA) following the manufacturer's instructions. The experiment was performed in three biological and two technical replicates. The average LDH release values obtained from the control condition was set to 100% and the relative LDH release levels for each treatment condition was compared to the control condition ($p < 0.05$).

2.3. Apoptosis

The rate of apoptosis in each treatment condition was measured using the TUNEL assay (Dead End Fluorimetric Kit, Promega, USA) following the manufacturer's instruction. The TUNEL positive cells (FITC) were counted in the growth plate zones as a percentage of all cells (FITC and DAPI) in each zone. The average percentage of TUNEL positive cells in each condition was obtained from 10 different zones under fluorescent microscope and data were analyzed using One Way ANOVA statistical test.

2.4. Protein sample preparation and 2-DE gel electrophoresis

Protein sample preparation and 2-DE gel electrophoresis were performed as described before (Jami et al., 2014b). Triplicate batches of SH-SY5Y cells were seeded at 20–30% confluence and harvested when cell density reached 90%. A total amount of 850 μg of soluble proteins in the sample buffer was loaded onto 24-cm IPG strips (GE Healthcare), with non-linear (NL) pH 3–11 gradient. Focusing of proteins, equilibration and the 12.5% SDS-PAGE for the second dimension were performed as previously described (Jami et al., 2010b). Briefly, Proteins were focused at 20 °C according to the following program: 1 h, 0 V and 12 h, 30 V (rehydration); 30-min gradient to 10,000 V; up to 9 h, 10,000 V until 85 kV-h. Gels were stained with Colloidal Coomassie (CC) following the "blue silver" staining method (Jami et al., 2010a), (Candiano et al., 2004).

2.5. Analysis of differential protein abundance

Two-dimensional images were captured by scanning, digitalizing and analysing stained gels as described previously (García-Estrada et al., 2013). Briefly, images were captured using an Image Scanner II (GE Healthcare) previously calibrated by using a gray scale marker (Eastman Kodak Co.), digitalized with Labscan 5.00 (v1.0.8) software (GE Healthcare), and analyzed with the Image Master TM 2D Platinum V7.0 software (GE Healthcare). Three gels for each condition, obtained from three independent cultures (biological replicates), were analysed to guarantee representative results. Differentially expressed proteins between two conditions were considered when the ratio of the relative volume average for one specific spot (present in the three biological replicates) was higher than 1.5 and the p-value was <0.05. False discovery rate (FDR) correction for multiple hypothesis testing was performed according to Storey's method (q-value < 0.05) (Storey, 2002).

2.6. Protein identification by mass spectrometry

The protein spots of interest were manually excised from the gel and washed three times with ammonium bicarbonate/acetonitrile 1:1 (vol/vol) solution. Polyacrylamide fragments were dehydrated in acetonitrile and dried with a vacuum concentrator. Protein

reduction and alkylation were performed by reswelling poly-acrylamide fragments in 25 mM ammonium carbonate containing 0.15 mg/ml DTT at 56 °C. This solution was replaced by 25 mM ammonium bicarbonate containing 10 mg/ml 2-iodoacetamide (Bio-Rad) for 45 min at room temperature and in the dark. Fragments were dried as described above and tryptic cleavage was initiated by reswelling the gel in 25 mM ammonium bicarbonate containing 0.2 µg trypsin per gel slice (Promega, WI, USA) for 20 min on ice. The solution was then replaced by 25 mM ammonium carbonate and digestion carried out overnight at 37 °C. Tryptic peptides were extracted at 37 °C for 15 min with a 50% (vol/vol) acetonitrile and 10% (vol/vol) acetic acid solution. A second extraction was performed under the same conditions. A third extraction was performed at room temperature for 15 min with 100% acetonitrile. The pooled solution was dried under vacuum and resuspended in 10 µl 0.1% (vol/vol) formic acid as described previously (Kosalková et al., 2012) with some modifications.

Five microliters of each sample were loaded onto a 75 µm × 15 cm column self-packed with 3 µm ReproSil-Pur C18-AQ beads (Dr. Maisch GmbH, Germany). Peptides were eluted with a gradient of 3–30% acetonitrile in 0.1% formic acid over 60 min at a flow rate of 250 nL/min at 45 °C using a Thermo Scientific EASY-nLC 1000 coupled to a Q Exactive mass spectrometer (Thermo Fisher Scientific). The Q Exactive was operated in data-dependent analysis mode with survey scans acquired at a resolution of 70,000. Up to the top 10 most abundant precursors from the survey scan were selected with an isolation window of 1.6 Thompsons and fragmented by higher-energy collisional dissociation with normalized collision energies of 27. The maximum ion injection times for the survey scan and the MS/MS scans were 20 ms and 60 ms, respectively, and the ion target value for the survey scan and the MS/MS scans was set to 3,000,000 and 1,000,000, respectively. The raw files were processed using the MaxQuant (Cox and Mann, 2008) computational proteomics platform (version 1.2.7.0) for peptide identification and quantitation. The fragmentation spectra were searched against the UniProt human protein database (downloaded June 27, 2014) containing 87,938 protein sequences and allowing up to two missed tryptic cleavages. Carbamidomethylation of cysteine was set as a fixed modification and oxidation of methionine and protein N-terminal acetylation were used as variable modifications for database searching. The precursor and fragment mass tolerances were set to 7 and 20 ppm, respectively. Both peptide and protein identifications were filtered at 1% false discovery rate (FDR) and thus were not dependent on the peptide score.

3. Results and discussion

3.1. Treatment conditions

To gain insight into the mechanism by which Edaravone influences the toxic effects of H_2O_2 in neuronal cells we performed three simultaneous treatments (each one in three biological replicates) on dopaminergic SH-SY5Y neuroblastoma cells and analyzed their proteomic profiles under four conditions: Condition 1 (control condition) contained cells grown in standard culture medium without treatment, condition 2 contained cells exposed to a toxic level (2 mM) of H_2O_2, condition 3 contained cells supplemented with 25 µM Edaravone, and condition 4 contained cells exposed to 25 µM Edaravone and 2 mM H_2O_2 simultaneously. Several studies have demonstrated that Edaravone concentrations, ranging from 1 to 100 µM, has no effect on cell viability (Lee et al., 2010) and because of this we chose a concentration of 25 µM for our experiments as this concentration resulted in a reversal of H_2O_2-induced cytotoxicity (Fig. 1).

3.2. Oxidative conditions modify cell morphology, cell integrity, and apoptosis rate

As shown in Fig. 1 the cell viability and morphology was clearly altered in response to toxic level of H_2O_2 in condition 2, however co-treatment of the culture media with Edaravone and H_2O_2 (in condition 4) prevented the viability and morphological changes (Fig. 1).

Similar results were observed by the Lactate dehydrogenase (LDH) Cytotoxicity assay that showed a significant increase (p < 0.05) in LDH levels released in the culture media in condition 2 (2.69 fold) and condition 4 (1.34 fold) compared to the control condition (Fig. 2). This finding demonstrated a cytotoxic role of H_2O_2 and a cytoprotective role for Edaravone as it decreased the cellular damage rate from 2.69 fold to 1.34.

In addition, TUNEL assays were performed to estimate the impact of different treatment condition on cell viability and apoptotic characteristics. These experiments showed averages of 0.84%, 19.38%, 1.32% and 4.83% of apoptotic cells in conditions 1, 2, 3 and 4 respectively (Fig. 3). The results of these experiment indicate significantly increased apoptosis in the presence of H_2O_2 (conditions 2 and 4) and further that Edaravone causes a significant decrease in apoptosis from 19.38% in condition 2–4.83% in condition 4.

3.3. Oxidative conditions affect the proteomic profile

The first set of proteomic analyses (condition 1 vs. condition 2) focused on the effects of H_2O_2, wherein we compared the proteome profile of SH-SY5Y cells under control condition (Fig. 4A) to cells treated with H_2O_2 (Fig. 4B). In the second set (condition1 vs. condition 3) we analyzed the effects of Edaravone exposure on SH-SY5Y cells (Fig. 5A) and in the third set (condition1 vs. condition 4) we analyzed the effects of simultaneous exposure to H_2O_2 and Edaravone (Fig. 5B). We evaluated the effects of H_2O_2 treatment on the cells in three conditions (conditions 1, 2 and 4, Figs. 4A, B and 5B) and observed an up-regulation of 10 proteins (spots1–6 and 10–13) and down-regulation of 6 proteins (7–9 and 14–16) compared to control condition (Table 1), the same result as we observed in our previous study (Jami et al., 2014b).

When comparing the proteome profiles of cells exposed to Edaravone (either with or without H_2O_2) to controls, we observed up-regulation of spot 17 (in condition 3) and down-regulation of spot 18 in condition 4. Detailed information on each protein change are summarized in Table 1 where we classify the differentially expressed proteins according to their gene ontology (GO, with focus on biological process) through Uniprot (protein knowledge website: http://www.uniprot.org/) and QuickGO (http://www.ebi.ac.uk/QuickGO/). Upon treatments, several biological processes were affected. For example the majority of protein changes in response to oxidative stress (conditions 2) belong to the "cell motion (GO:0006928)" category of proteins, most of which were prevented by Edaravone co-treatment (condition 4).

3.4. Oxidative stress alters proteins involved in the metabolic routes to generate higher levels of NADPH

Glutathione is one of the main cellular antioxidants that prevents damage caused by ROS (Pompella et al., 2003). During the conversion of reactive H_2O_2 into H_2O the reduced form of glutathione is oxidized by glutathione peroxidase. Then glutathione reductase and NADPH are required to reduce the oxidized glutathione back to its reduced form. Similar to our findings in our previous study, neurons seem to respond to the oxidative stress by generation of higher levels of NADPH (Jami et al., 2014b). One major
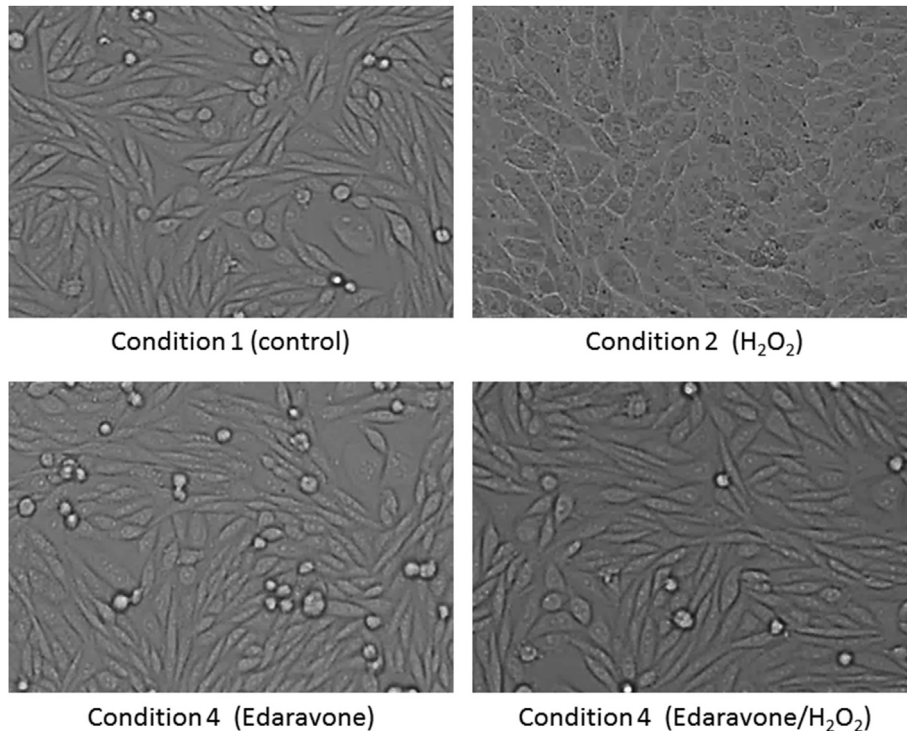
Fig. 1. Morphology of SH-SY5Y cells during treatments. SH-SY5Y cells have normal morphology in both condition 1 (without treatment) and condition 3 (treatment with 25 μM Edaravone for 8 h). Cellular morphology is altered in response to treatment 2 (2 mM H_2O_2 for 8 h). Normal cellular morphology is maintained in condition 4 (2 mM H_2O_2 and 25 μM Edaravone for 8 h).
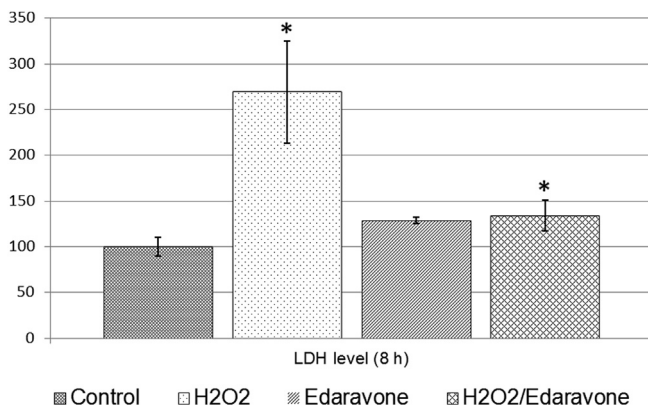

Fig. 2. Lactate dehydrogenase (LDH) Cytotoxicity assay. Cellular damage following each treatment condition was assessed by measurement of LDH released into the medium solution. The average LDH release values obtained from the control condition was set to 100% and the relative LDH release levels for each treatment condition was compared to the control condition. LDH levels released in the culture media significantly increased ($p < 0.05$) in condition 2 (2.69 fold) and condition 4 (1.34 fold).

observation in our work is the down regulation of glyceraldehyde 3-phosphate dehydrogenase (GAPDH). This alteration can result in a metabolic flux change from glycolysis to the pentose phosphate pathway (PPP) (Ralser et al., 2007; Jami et al., 2014a). PPP allows cells to produce higher levels of NADPH to overcome the oxidative conditions and prevent damage caused by ROS (Pompella et al., 2003).

We also observed that lactate dehydrogenase (LDH), involved in oxidation-reduction is up-regulated, a finding that is in concordance with the results of our LDH cytotoxicity assay. As a cytosolic enzyme, LDH catalyzes the conversion of pyruvate to lactate in the absence of oxygen, however it can also perform the reverse reaction in oxidative conditions and generate NADH (Markert, 1984).

We detected a marked up-regulation of mitochondrial nucleoside-diphosphate kinase and fumarate hydratase, both involved in the tricarboxylic acid (TCA) cycle that generates NADH (convertible to NADPH via nicotinomide nucleotide transhydrogenase (NNT)). Our analysis also showed up-regulation of 3-Hydroxyacyl CoA dehydrogenase, an oxidoreductase enzyme involved in beta-oxidation of fatty acids, catalyzing the oxidation of L-3-hydroxyacyl CoA by NAD+ thus generating NADH in response to oxidative stress (Table 1).

3.5. Cell survival mechanisms are activated in response to oxidative conditions

In all of the oxidative stress conditions tested we observed down-regulation of Cathepsin X and Cyclophilin D (both involved in cell death) and up-regulation of three stress sensor proteins (Table 1): Annexin A1, Peroxiredoxin-6 and PARK7/DJ-1. All of these three proteins are involved in cell survival; Annexin A1 can directly improve cell survival by limiting excessive levels of ROS during oxidative stress (Gorecka et al., 2005), Peroxiredoxin-6 can reduce H_2O_2, short chain fatty acids and phospholipid hydroperoxides (Fisher, 2011) and PARK7/DJ-1 is involved in protecting cells against oxidative stress and cell death (Ariga et al., 2013).

3.6. Oxidative conditions affect proteins responsible for cell integrity

We observed cell morphology modification (Fig. 1) and significant cell damage (Fig. 2) in condition 2 containing toxic level of H_2O_2 mostly in the absence of Edaravone. Interestingly, the
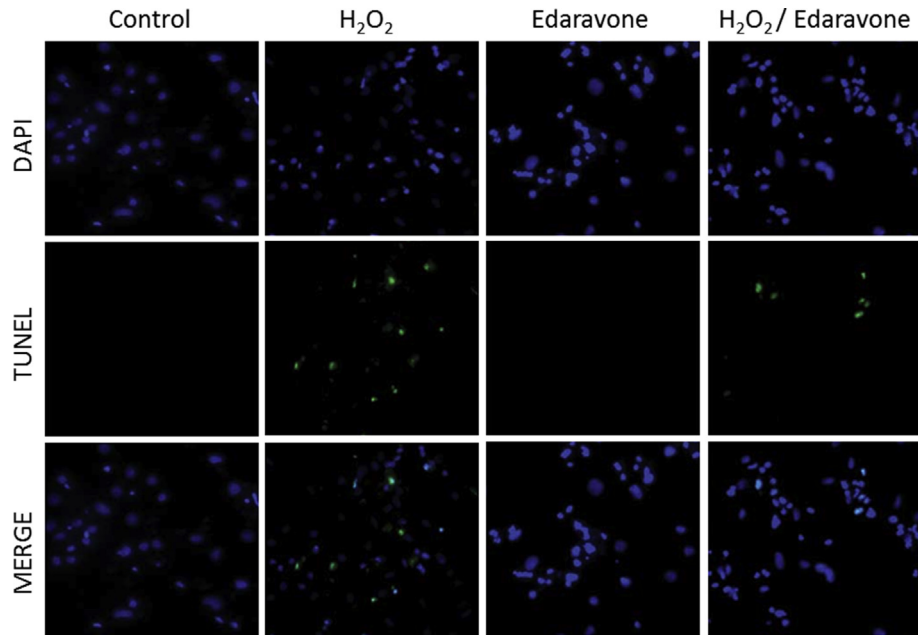
Fig. 3. Evaluation of apoptosis using the TUNEL assay. The different images illustrate representative zones from each condition stained by DAPI, TUNEL. The merged images are also shown. The average percentage of TUNEL positive cells from 10 different zones in each treatment condition was 0.84%, 19.38%, 1.32% and 4.83% in conditions 1, 2, 3 and 4 respectively.
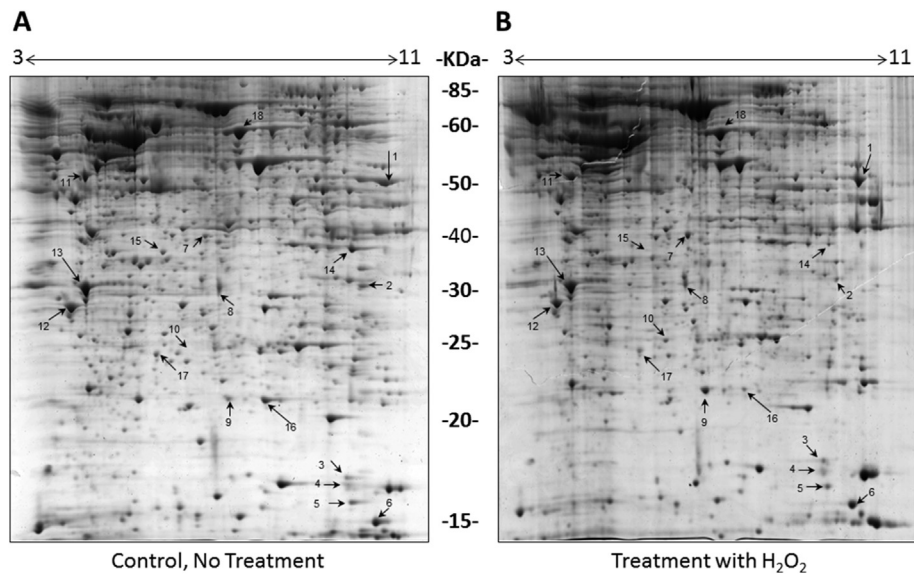

Fig. 4. Comparison of the proteomes of SH-SY5Y cells with or without H_2O_2. Representative 2-DE gels (n = 3 for each treatment) of the proteomes of SH-SY5Y cells grown for 8 h in the absence (A) or presence (B) of 2 mM H_2O_2. Protein spots showing differential abundance between the two conditions are numbered and correspond to the proteins listed in Table 1.

alteration of several structural proteins indicates a rearrangement of the cytoskeleton due to oxidative stress. For instance, while all three members of the ADF/cofilin family, including Cofilin-1 and Cofilin-2 (which control actin polymerization/depolymerization in a pH-sensitive manner (Bravo-Cordero et al., 2013)) and Destrin (an actin depolymerizing factor) are up-regulated, other actin binding proteins, such as Tropomyosin alpha-4 chain and Tropomyosin alpha-1 chain are down-regulated (Table 1). These proteins bind to actin filaments in muscle and non-muscle cells and play a central role in muscle contraction and in stabilizing cytoskeleton actin filaments in non-muscle cells (Lin et al., 2008).

Down-regulation of Vimentin, that is responsible for maintaining cell shape, cytoplasmic integrity, and stabilization of cytoskeletal interactions, is also interesting (Table 1). This protein is known to play a pivotal role in anchoring organelles in the cytosol (Goldman et al., 1996; Katsumoto et al., 1990). It is possible therefore that the observed neuronal morphological changes in response to H_2O_2, are due to the attenuation of Vimentin.

3.7. Cytotoxic effects of oxidative stress is reversed by Edaravone

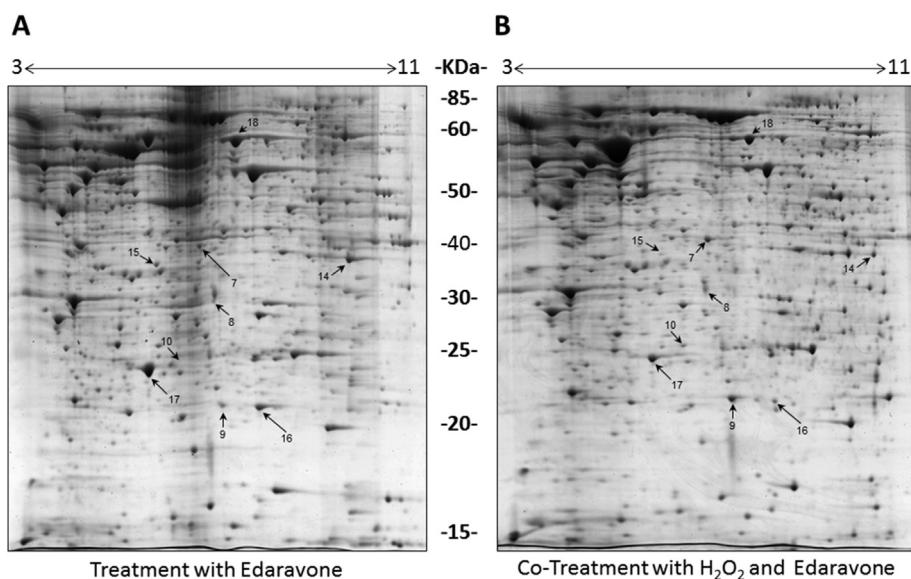Our proteomic analyses show that the alteration of three

Fig. 5. Proteomes of SH-SY5Y cells exposed to Edaravone with or without H_2O_2. Representative 2-DE gels (n = 3 for each treatment) of the proteomes of SH-SY5Y cells grown in media containing 25 μM Edaravone for 8 h in the absence (A) or presence (B) of 2 mM H_2O_2. Protein spots showing differential abundance between the two conditions are numbered and correspond to the proteins listed in Table 1.

mitochondrial enzymes under oxidative stress condition (fumarate hydratase, nucleoside-diphosphate kinase and 3-Hydroxyacyl CoA dehydrogenase) is maintained at baseline in response to Edaravone co-treatments (Table 1). Furthermore, we observed the ability of Edaravone in preventing the toxic effects of H_2O_2 on cellular integrity (Figs. 1 and 2). This is in concert with our proteomic results indicating that Edaravone co-treatments maintained the expression levels of spots 3, 4, 5, 7, 8 and 9 (the H_2O_2-induced protein alterations affecting the cytoskeleton) at baseline (Figs. 4 and 5, Table 1) and is also similar to the results of our previous study where we observed cytoprotective effects of L-Dopa against oxidative stress (Jami et al., 2014b).

3.8. Edaravone protects against oxidative stress through Peroxiredoxin-2

Edaravone treatment resulted in a large increase in the levels of Peroxiredoxin-2 (PRX2, spot 17 with an average of 12.69 fold overexpression) (Table 1). Interestingly, the largest increase in PRX2 is observed in response to Edaravone treatment (conditions 3) whilst the PRX2 induction (5.88 fold), although higher than control conditions, decreases in response to simultaneous Edaravone and H_2O_2 treatment (condition 4) (Fig. 5). This finding suggests that Edaravone scavenges H_2O_2 via induction of PRX2 and that PRX2 may be degraded during oxidative stress condition.

Peroxiredoxins (PRXs) represent one of the ROS management systems that maintain the intracellular reducing environment via redox reactions at certain cysteine residues. Among them, PRX2 levels are known to be significantly elevated in the substantia nigra of PD patients (Basso et al., 2004). Since PRX2 is the most abundant PRX enzyme in mammalian neurons (Jin et al., 2005), PRX2 is considered a vital PRX in DA neuronal survival protecting cells against oxidative stress (Stresing et al., 2013). It has been documented that PRX2 is inactivated by hyperoxidation during the elimination of peroxides (Peskin et al., 2013).

PRX2 is also known to protect cells against oxidative dopaminergic neurodegeneration via attenuation of the apoptosis signal-regulating kinase (ASK1) signaling cascade; this protein inhibits

ASK1 activity and the subsequent activation of JNK/c-Jun and p38 cell death pathways (Hu et al., 2011).

The catalytic breakdown of H_2O_2 by typical 2-Cys PRXs is conducted by oxidation of the peroxide-reactive peroxidatic cysteine followed by the formation of a disulfide with the resolving cysteine of a neighboring PRX molecule (Day et al., 2012). Thioredoxin then reduces this disulfide to restore the active peroxidase. In addition to its role in the catalytic cycle of PRX, thioredoxin is a cofactor for many other enzymes and its oxidoreductase activity is important for reduction of protein disulfides under oxidative stress conditions (Day et al., 2012). Interestingly, in our proteomic analyses we observed that the protein disulfide-isomerase A3 or PDIA3 protein is down-regulated (spot 18, 0.28 fold) upon co-treatment of cells with Edaravone and H_2O_2 (Table 1). The PDIA3 protein belongs to the protein disulfide isomerase family and catalyzes the rearrangement of -S-S- bonds in proteins (Bourdi et al., 1995). Our bioinformatics analysis using BioGraph online software (http://biograph.be/)(Liekens et al., 2011) revealed that this protein contains 2 thioredoxin domains and can therefore participate in redox regulation through the thioredoxin/peroxiredoxin system. Moreover, it has been reported that inhibition of PDIA3, as a pro-apoptotic protein that catalyzes isomerization, reduction, and oxidation of disulfides, can suppress apoptosis suggesting increased neuronal survival (Hoffstrom et al., 2010).

This knowledge combined with our experimental findings suggests that Edaravone protects neuronal cells against oxidative stress either by inhibition of apoptosis or more specifically via direct induction of PRX2. The exact mechanism of Edaravone-mediated neuroprotection warrants further investigation as Edaravone may not only be a potent neuroprotective agent following acute brain ischemia, but also as a component of future combinatorial PD therapeutic strategies. In our previous study we showed that L-Dopa reverses the H_2O_2-mediated effects at the cell morphology and viability level via indirect induction of the ORP150 protein. Since conversion of L-Dopa to norepinephrine requires molecular oxygen, the exposure to L-Dopa may aid hypoxia condition in cells and therefore induction of ORP150 with its concomitant cytoprotective effects (Jami et al., 2014b).

Table 1
Detailed information on altered spots during treatment conditions. Differentially expressed proteins (fold-change higher than 1.5 and p-value < 0.05) were classified according to their gene ontology (GO). Several biological processes were affected.

Spot ID	Protein ID	Description	Mass	PI	Score	Percent protein coverage	AVG fold change	p-value	q-value	GO (biological process)
1	P07954	Fumarate hydratase, mitochondrial	54714	8.85	408	27.2	7.49	3.30E-03	1.42E-04	GO:0009056~catabolic process, GO:0042592~homeostatic process
2	Q16836	Hydroxyacyl-coenzyme A dehydrogenase	34613	8.76	118	21.5	5.1	4.52E-03	1.48E-03	GO:0055114~oxidation reduction
3	Q9Y281	Cofilin-2	18764	7.66	113	33.1	7.1	8.17E-04	1.63E-03	GO:0030042~actin filament depolymerization
4	P60981	Destrin	18852	8.14	147	26.1	4.44	1.33E-04	1.71E-03	GO:0006928~cell motion, GO:0043243~positive regulation of protein complex disassembly
5	P23528	Cofilin-1	18776	8.22	192	50.6	4.3	2.87E-04	1.86E-03	GO:0006928~cell motion, GO:0043243~positive regulation of protein complex disassembly
6	O00746	Nucleoside diphosphate kinase	17469	7.77	1024	41.4	2.7	3.02E-03	2.03E-03	GO:0009116~nucleoside metabolic process
7	Q9BYZ2	L-lactate dehydrogenase A-like 6B	36817	7.62	244	29.6	4.15	1.71E-02	3.82E-03	GO:0055114~oxidation reduction, GO:0006096~glycolysis
8	P04083	Annexin A1	38816	6.57	142	6.62	2.07	3.78E-03	4.26E-03	GO:00070301~cellular response to hydrogen proxide, GO:0006954~inflammatory response
9	Q99497	Protein DJ-1	20064	6.33	501	21.2	8.52	7.77E-04	4.15E-03	GO:0006979~response to oxidative stress, GO:0042592~homeostatic process
10	P30041	Peroxiredoxin-6	25109	5.74	348	35.7	11.3	3.10E-04	4.95E-03	GO:0009056~catabolic process, GO:0055114~oxidation reduction
11	P08670	Vimentin	53754	5.06	1536	62.2	0.22	2.93E-03	5.00E-03	GO:0006928~cell motion
12	P67936	Tropomyosin alpha-4 chain	28620	4.65	138	23.8	0.16	1.74E-02	5.16E-03	GO:0006928~cell motion
13	P09493	Tropomyosin alpha-1 chain	32746	4.69	405	33.1	0.12	3.11E-03	5.65E-03	GO:0006979~response to oxidative stress, GO:0006928~cell motion, GO:0046907~intracellular transport
14	O14556	Glyceraldehyde-3-phosphate dehydrogenase,	35953	8.49	1165	48.6	0.17	6.76E-03	7.39E-03	GO:0055114~oxidation reduction, GO:0006096~glycolysis, GO:0006928~cell motion
15	Q9UBR2	Cathepsin Z	34658	6.13	308	15.7	0.15	8.00E-03	7.92E-03	GO:0006508~proteolysis
16	Q08752	Peptidyl-prolyl cis-trans isomerase D	20436	6.77	139	8.88	0.12	3.38E-04	8.38E-03	GO:0043065~positive regulation of apoptotic process
17	P32119	Peroxiredoxin-2	22049	5.66	140	24	12.69	9.64E-03	8.96E-03	GO:0032943~mononuclear cell proliferation, GO:0006979~response to oxidative stress, GO:0042592~homeostatic process
18	P30101	Protein disulfide-isomerase A3	57099	6.88	1573	52.7	0.28	3.38E-03	9.43E-03	GO:0042592~homeostatic process, GO:0046907~intracellular transport

4. Conclusions

Free radicals are important targets for therapeutic intervention of neurodegenerative diseases as oxidative stress represents an important factor. As a free radical scavenger, Edaravone may offer a novel treatment option for neurodegeneration. Using a 2DE-based proteomic study we have shown that oxidative stress changes neuronal metabolic routes and affects cytoskeletal integrity in neuroblastoma cells. As observed with L-Dopa in our previous study we show here that Edaravone reverses H_2O_2-mediated effects at the protein level. However, the cytoprotective effects of these two compounds appear to influence different pathways. L-Dopa seems to aid hypoxia condition in cells and therefore induction of ORP150 with its concomitant cytoprotective effects whilst Edaravone protect neuronal cells against oxidative stress via direct induction of PRX2 and inhibition of apoptosis.

Conflicts of interest

The authors declare that they have no conflict of interest.

Acknowledgements

References

Ariga, H., Takahashi-Niki, K., Kato, I., Maita, H., Niki, T., Iguchi-Ariga, S.M.M., 2013. Neuroprotective function of DJ-1 in Parkinson's disease. Oxidative Med. Cell. Longev. 2013, 683920. http://dx.doi.org/10.1155/2013/683920.

Basso, M., Giraudo, S., Corpillo, D., Bergamasco, B., Lopiano, L., Fasano, M., 2004. Proteome analysis of human substantia nigra in Parkinson's disease. Proteomics 4, 3943–3952. http://dx.doi.org/10.1002/pmic.200400848.

Blessing, H., Bareiss, M., Zettlmeisl, H., Schwarz, J., Storch, A., 2003. Catechol-O-methyltransferase inhibition protects against 3,4-dihydroxyphenylalanine (DOPA) toxicity in primary mesencephalic cultures: new insights into levo-dopa toxicity. Neurochem. Int. 42, 139–151.

Bosco, D.A., Fowler, D.M., Zhang, Q., Nieva, J., Powers, E.T., Wentworth, P., Lerner, R.A., Kelly, J.W., 2006. Elevated levels of oxidized cholesterol metabolites in Lewy body disease brains accelerate alpha-synuclein fibrilization. Nat. Chem. Biol. 2, 249–253. http://dx.doi.org/10.1038/nchembio782.

Bourdi, M., Demady, D., Martin, J.L., Jabbour, S.K., Martin, B.M., George, J.W., Pohl, L.R., 1995. cDNA cloning and baculovirus expression of the human liver endoplasmic reticulum P58: characterization as a protein disulfide isomerase isoform, but not as a protease or a carnitine acyltransferase. Archives Biochem. Biophys. 323, 397–403. http://dx.doi.org/10.1006/abbi.1995.0060.

Bravo-Cordero, J.J., Magalhaes, M.A.O., Eddy, R.J., Hodgson, L., Condeelis, J., 2013. Functions of cofilin in cell locomotion and invasion. Nat. rev. Mol. Cell Biol. 14, 405–415. http://dx.doi.org/10.1038/nrm3609.

Candiano, G., Bruschi, M., Musante, L., Santucci, L., Ghiggeri, G.M., Carnemolla, B., Orecchia, P., Zardi, L., Righetti, P.G., 2004. Blue silver: a very sensitive colloidal Coomassie G-250 staining for proteome analysis. Electrophoresis 25, 1327–1333. http://dx.doi.org/10.1002/elps.200305844.

Cox, J., Mann, M., 2008. MaxQuant enables high peptide identification rates, individualized p.p.b.-range mass accuracies and proteome-wide protein quantification. Nat. Biotechnol. 26, 1367–1372. http://dx.doi.org/10.1038/nbt.1511.

Davie, C.A., 2008. A review of Parkinson's disease. Br. Med. Bull. 86, 109–127. http://dx.doi.org/10.1093/bmb/ldn013.

Dawson, T.M., Ko, H.S., Dawson, V.L., 2010. Genetic animal models of Parkinson's disease. Neuron 66, 646–661. http://dx.doi.org/10.1016/j.neuron.2010.04.034.

Day, A.M., Brown, J.D., Taylor, S.R., Rand, J.D., Morgan, B.A., Veal, E.A., 2012. Inactivation of a peroxiredoxin by hydrogen peroxide is critical for thioredoxin-mediated repair of oxidized proteins and cell survival. Mol. Cell 45, 398–408. http://dx.doi.org/10.1016/j.molcel.2011.11.027.

De Lau, L.M.L., Breteler, M.M.B., 2006. Epidemiology of Parkinson's disease. Lancet Neurol. 5, 525–535. http://dx.doi.org/10.1016/S1474-4422(06)70471-9.

Dorsey, E.R., Constantinescu, R., Thompson, J.P., Biglan, K.M., Holloway, R.G., Kieburtz, K., Marshall, F.J., Ravina, B.M., Schifitto, G., Siderowf, A., Tanner, C.M., 2007. Projected number of people with Parkinson disease in the most populous nations, 2005 through 2030. Neurology 68, 384–386. http://dx.doi.org/10.1212/01.wnl.0000247740.47667.03.

Fisher, A.B., 2011. Peroxiredoxin 6: a bifunctional enzyme with glutathione peroxidase and phospholipase A_2 activities. Antioxid. Redox Signal. 15, 831–844. http://dx.doi.org/10.1089/ars.2010.3412.

García-Estrada, C., Barreiro, C., Jami, M.-S., Martín-González, J., Martín, J.-F., 2013. The inducers 1,3-diaminopropane and spermidine cause the reprogramming of metabolism in Penicillium chrysogenum, leading to multiple vesicles and penicillin overproduction. J. Proteomics 85, 129–159. http://dx.doi.org/10.1016/j.jprot.2013.04.028.

Goldman, R.D., Khuon, S., Chou, Y.H., Opal, P., Steinert, P.M., 1996. The function of intermediate filaments in cell shape and cytoskeletal integrity. J. Cell Biol. 134, 971–983.

Gorecka, K.M., Konopka-Postupolska, D., Hennig, J., Buchet, R., Pikula, S., 2005. Peroxidase activity of annexin 1 from Arabidopsis thaliana. Biochem. Biophys. Res. Commun. 336, 868–875. http://dx.doi.org/10.1016/j.bbrc.2005.08.181.

Hoffstrom, B.G., Kaplan, A., Letso, R., Schmid, R.S., Turmel, G.J., Lo, D.C., Stockwell, B.R., 2010. Inhibitors of protein disulfide isomerase suppress apoptosis induced by misfolded proteins. Nat. Chem. Biol. 6, 900–906. http://dx.doi.org/10.1038/nchembio.467.

Hu, X., Weng, Z., Chu, C.T., Zhang, L., Cao, G., Gao, Y., Signore, A., Zhu, J., Hastings, T., Greenamyre, J.T., Chen, J., 2011. Peroxiredoxin-2 protects against 6-hydroxydopamine-induced dopaminergic neurodegeneration via attenuation of the apoptosis signal-regulating kinase (ASK1) signaling cascade. J. Neurosci. Off. J. Soc. Neurosci. 31, 247–261. http://dx.doi.org/10.1523/JNEUROSCI.4589-10.2011.

Jami, M.-S., Barreiro, C., García-Estrada, C., Martín, J.-F., 2010a. Proteome analysis of the penicillin producer Penicillium chrysogenum: characterization of protein changes during the industrial strain improvement. Mol. Cell. Proteomics MCP 9, 1182–1198.

Jami, M.-S., García-Estrada, C., Barreiro, C., Cuadrado, A.-A., Salehi-Najafabadi, Z., Martín, J.-F., 2010b. The Penicillium chrysogenum extracellular proteome. Conversion from a food-rotting strain to a versatile cell factory for white biotechnology. Mol. Cell. Proteomics MCP 9, 2729–2744.

Jami, M.-S., Hou, J., Liu, M., Varney, M.L., Hassan, H., Dong, J., Geng, L., Wang, J., Yu, F., Huang, X., Peng, H., Fu, K., Li, Y., Singh, R.K., Ding, S.-J., 2014a. Functional proteomic analysis reveals the involvement of KIAA1199 in breast cancer growth, motility and invasiveness. BMC Cancer 14, 194. http://dx.doi.org/10.1186/1471-2407-14-194.

Jami, M.-S., Pal, R., Hoedt, E., Neubert, T.A., Larsen, J.P., Møller, S.G., 2014b. Proteome analysis reveals roles of L-DOPA in response to oxidative stress in neurons. BMC Neurosci. 15, 93. http://dx.doi.org/10.1186/1471-2202-15-93.

Jin, M.-H., Lee, Y.-H., Kim, J.-M., Sun, H.-N., Moon, E.-Y., Shong, M.H., Kim, S.-U., Lee, S.H., Lee, T.-H., Yu, D.-Y., Lee, D.-S., 2005. Characterization of neural cell types expressing peroxiredoxins in mouse brain. Neurosci. Lett. 381, 252–257. http://dx.doi.org/10.1016/j.neulet.2005.02.048.

Kaste, M., Murayama, S., Ford, G.A., Dippel, D.W.J., Walters, M.R., Tatlisumak, T., 2013. Safety, tolerability and pharmacokinetics of MCI-186 in patients with acute ischemic stroke: new formulation and dosing regimen. Cerebrovasc. Dis. (Basel, Switzerland) 36, 196–204. http://dx.doi.org/10.1159/000353680.

Katsumoto, T., Mitsushima, A., Kurimura, T., 1990. The role of the vimentin intermediate filaments in rat 3Y1 cells elucidated by immunoelectron microscopy and computer-graphic reconstruction. Biol. Cell/Under Auspices Eur. Cell Biol. Organ. 68, 139–146.

Kikuchi, K., Tanaka, E., Murai, Y., Tancharoen, S., 2014. Clinical trials in acute ischemic stroke. CNS Drugs 28, 929–938. http://dx.doi.org/10.1007/s40263-014-0199-6.

Kiyoshi, K., Kiyoshi, K., Naoki, M., Yoko, M., Takashi, I., Salunya, T., Kei, M., Chiemi, K., Narumi, I., Nobuyuki, T., Hisaaki, U., Naohisa, M., Naoto, S., Terukazu, K., Teruto, H., Ikuro, M., Motohiro, M., Ko-ichi, K., 2011. Beneficial effects of the free radical scavenger edaravone (Radicut) in neurologic diseases. J. Neurol. Neurophysiol. http://dx.doi.org/10.4172/2155-9562.S1-001. Special issue 1.

Kosalková, K., García-Estrada, C., Barreiro, C., Flórez, M.G., Jami, M.S., Paniagua, M.A., Martín, J.F., 2012. Casein phosphopeptides drastically increase the secretion of extracellular proteins in Aspergillus awamori. Proteomics studies reveal changes in the secretory pathway. Microb. Cell Factor. 11, 5. http://dx.doi.org/10.1186/1475-2859-11-5.

Lapchak, P.A., 2010. A critical assessment of edaravone acute ischemic stroke efficacy trials: is edaravone an effective neuroprotective therapy? Expert Opin. Pharmacother. 11, 1753–1763. http://dx.doi.org/10.1517/14656566.2010.493558.

Lee, B.J., Egi, Y., van Leyen, K., Lo, E.H., Arai, K., 2010. Edaravone, a free radical scavenger, protects components of the neurovascular unit against oxidative stress in vitro. Brain Res. 1307, 22–27. http://dx.doi.org/10.1016/j.brainres.2009.10.026. Epub 2009 Oct 17.

Liekens, A.M.L., De Knijf, J., Daelemans, W., Goethals, B., De Rijk, P., Del-Favero, J., 2011. BioGraph: unsupervised biomedical knowledge discovery via automated hypothesis generation. Genome Biol. 12, R57. http://dx.doi.org/10.1186/gb-2011-12-6-r57.

Lin, J.J.-C., Eppinga, R.D., Warren, K.S., McCrae, K.R., 2008. Human tropomyosin isoforms in the regulation of cytoskeleton functions. Adv. Exp. Med. Biol. 644, 201–222.

Liu, X., Shao, R., Li, M., Yang, G., 2014. Edaravone protects neurons in the rat substantia nigra against 6-hydroxydopamine-induced oxidative stress damage. Cell Biochem. Biophys. 70, 1247–1254. http://dx.doi.org/10.1007/s12013-014-0048-8.

Markert, C.L., 1984. Lactate dehydrogenase. Biochemistry and function of lactate dehydrogenase. Cell Biochem. Funct. 2, 131–134. http://dx.doi.org/10.1002/cbf.290020302.

Mena, M.A., Casarejos, M.J., Solano, R.M., de Yébenes, J.G., 2009. Half a century of L-DOPA. Curr. Top. Med. Chem. 9, 880–893.

Nakabeppu, Y., Tsuchimoto, D., Yamaguchi, H., Sakumi, K., 2007. Oxidative damage in nucleic acids and Parkinson's disease. J. Neurosci. Res. 85, 919–934. http://dx.doi.org/10.1002/jnr.21191.

Peskin, A.V., Dickerhof, N., Poynton, R.A., Paton, L.N., Pace, P.E., Hampton, M.B., Winterbourn, C.C., 2013. Hyperoxidation of peroxiredoxins 2 and 3: rate constants for the reactions of the sulfenic acid of the peroxidatic cysteine. J. Biol. Chem. 288 (20), 14170–14177. http://dx.doi.org/10.1074/jbc.M113.460881.

Pompella, A., Visvikis, A., Paolicchi, A., De Tata, V., Casini, A.F., 2003. The changing faces of glutathione, a cellular protagonist. Biochem. Pharmacol. 66, 1499–1503.

Ralser, M., Wamelink, M.M., Kowald, A., Gerisch, B., Heeren, G., Struys, E.A., Klipp, E., Jakobs, C., Breitenbach, M., Lehrach, H., Krobitsch, S., 2007. Dynamic rerouting of the carbohydrate flux is key to counteracting oxidative stress. J. Biol. 6, 10. http://dx.doi.org/10.1186/jbiol61.

Shinohara, Y., Inoue, S., 2013. Cost-effectiveness analysis of the neuroprotective agent edaravone for noncardioembolic cerebral infarction. J. Stroke Cerebrovasc. Dis. Off. J. Natl. Stroke Assoc. 22, 668–674. http://dx.doi.org/10.1016/j.jstrokecerebrovasdis.2012.04.002.

Storey, J.D., 2002. A direct approach to false discovery rates. J. R. Stat. Soc. Ser. B (Statistical Methodology) 64, 479–498. http://dx.doi.org/10.1111/1467-9868.00346.

Stresing, V., Baltziskueta, E., Rubio, N., Blanco, J., Arriba, M.C., Valls, J., Janier, M., Clézardin, P., Sanz-Pamplona, R., Nieva, C., Marro, M., Petrov, D., Dmitri, P., Sierra, A., 2013. Peroxiredoxin 2 specifically regulates the oxidative and metabolic stress response of human metastatic breast cancer cells in lungs. Oncogene 32, 724–735. http://dx.doi.org/10.1038/onc.2012.93.

Yamamoto, Y., Yanagisawa, M., Tak, N.W., Watanabe, K., Takahashi, C., Fujisawa, A., Kashiba, M., Tanaka, M., 2009. Repeated edaravone treatment reduces oxidative cell damage in rat brain induced by middle cerebral artery occlusion. Redox Rep. Commun. Free Radic. Res. 14, 251–258. http://dx.doi.org/10.1179/135100009X12525712409779.

Yoshida, H., Yanai, H., Namiki, Y., Fukatsu-Sasaki, K., Furutani, N., Tada, N., 2006. Neuroprotective effects of edaravone: a novel free radical scavenger in cerebrovascular injury. CNS Drug Rev. 12, 9–20. http://dx.doi.org/10.1111/j.1527-3458.2006.00009.x.

Zeevalk, G.D., Razmpour, R., Bernard, L.P., n.d. Glutathione and Parkinson's disease: is this the elephant in the room? Biomed. Biomédecine pharmacothérapie 62, 236–249. doi:10.1016/j.biopha.2008.01.017.

Zhao, Z.-Y., Luan, P., Huang, S.-X., Xiao, S.-H., Zhao, J., Zhang, B., Gu, B.-B., Pi, R.-B., Liu, J., 2013. Edaravone protects HT22 neurons from H2O2-induced apoptosis by inhibiting the MAPK signaling pathway. CNS Neurosci. Ther. 19, 163–169. http://dx.doi.org/10.1111/cns.12044.